*Tumor and Stem Cell Biology*

Cancer Research

# Inhibition of Stathmin1 Accelerates the Metastatic Process

Karin Williams[1], Ritwik Ghosh[3], Premkumar Vummidi Giridhar[1], Guangyu Gu[5], Thomas Case[4], Scott M. Belcher[2], and Susan Kasper[1]

## Abstract

The oncoprotein stathmin 1 (STMN1) is upregulated in most, if not all, cancers of epithelial cell origin; therefore STMN1 is considered a target for cancer therapy. However, its role during metastasis has not been investigated. Here, we report for the first time that STMN1 strongly inhibits metastatic behavior in both normal epithelial and cancerous epithelial cells. Initially, loss-of-STMN1 compromises cell–cell adhesion. This is followed by epithelial-to-mesenchymal transition (EMT), increased cell migration, and metastasis via cooperative activation of p38 and through TGF-β–independent and -dependent mechanisms. In contrast, expressing STMN1 restores cell–cell adhesion and reverses the metastatic cascade. Primary prostate epithelial cell cultures from benign to undifferentiated adenocarcinoma (UA) clinical biopsies show that EMT-like cells arise while the cancer is still organ-confined and that their emergence is tumor-stage specific. Furthermore, primary EMT-like cells exhibit metastatic behavior both *in vitro* and *in vivo* as compared with their non-EMT counterpart. These observations predict that using STMN1 as a generic therapeutic target might accelerate metastasis. Instead, there may be a tumor stage-specific window-of-opportunity in which conserving STMN1 expression is required to inhibit emergence of metastatic disease. *Cancer Res; 72(20); 5407–17. ©2012 AACR.*

## Introduction

The oncoprotein stathmin (STMN1) has been identified in profiling signatures of many cancers ranging from prostate, breast, and colorectal cancers to pheochromocytomas and multiple myeloma (1–5). Increased STMN1 expression correlates with disease progression and poor prognostic outcome (6). Therefore, it has gained considerable interest as a prognostic marker and potential therapeutic target (7). STMN1 is a phosphoprotein, which regulates cell spindle formation and microtubule dynamics (8). Dephosphorylation activates STMN1, resulting in microtubule disassembly through the binding of 2 α,β-tubulin heterodimers per STMN1 molecule (9). This step is critical during late metaphase/anaphase in which rapid STMN1 dephosphorylation prevents cells from reentering the cell cycle (10). In contrast, phosphorylation of STMN1 at serine residues $Ser^{16}$, $Ser^{25}$, $Ser^{38}$, and $Ser^{63}$ inactivates STMN1 by reducing its interaction with tubulin, thereby increasing free α,β-tubulin heterodimers and promoting microtubule assembly (11–13). During initiation of mitosis, STMN1 phosphorylation is required for mitotic spindle assembly (14). On the basis of these observations, it is postulated that oncogenesis may arise through constitutive STMN1 phosphorylation or decreased protein expression, which deregulates spindle formation and promotes cell-cycle progression (14).

A further mechanism in which STMN1 may be oncogenic is through regulation of cytoskeletal dynamics during epithelial-to-mesenchymal transition (EMT) and cell migration. In migrating cells, STMN1 is locally inactivated at the leading edge of the cell to allow localized microtubule growth down a gradient of phosphorylated stathmin (15). Collectively, these observations imply that both promotion of cell-cycle progression and EMT requires phosphorylation and subsequent inhibition of STMN1 activity.

STMN1 is phosphorylated in response to p38 and its activity is inhibited by treatment with the p38 inhibitor SB203580 (16, 17). In MDA-MB-231 cells, p38 signaling enhances cell migration (18), whereas a ternary complex formed by $Ca^{2+}$/calmodulin–dependent protein kinase II (CaMK II), Siva1, and STMN1 results in STMN1 phosphorylation at $Ser^{16}$, weakened STMN1–α-tubulin interactions, and inhibition of EMT and cell migration (19). Furthermore, p38 promotes EMT through TGF-β–independent and/or TGF-β–dependent signaling (20–22). Whether MAP kinase signaling directly downregulates STMN1 to promote EMT through either TGF-β–dependent or -independent mechanisms remains to be determined.

On the basis of these previous studies, it seems that inactivation of STMN1, and not overexpression and/or increased STMN1 activity, is key to promoting oncogenesis and EMT. Therefore, a conundrum exists between the observations that increased STMN1 expression correlates with oncogenesis and disease progression, and decreased STMN1 activity promotes oncogenesis and EMT. We initiated the following study to elucidate whether STMN1 exhibited oncogenic or metastasis suppressor activity. Our study shows that loss-of-STMN1

**Authors' Affiliations:** Departments of [1]Environmental Health, [2]Pharmacology & Cell Biophysics, University of Cincinnati, Cincinnati, Ohio; Departments of [3]Medicine, [4]Urologic Surgery, Vanderbilt University School of Medicine, Nashville, Tennessee; and [5]Department of Pathology, ARUP Laboratories/University of Utah, Salt Lake City, Utah

K. Williams and R. Ghosh contributed equally to this work.

**Corresponding Author:** Susan Kasper, School of Medicine, 3223 Eden Av., Kettering Lab Complex, Rm 267, Cincinnati, OH 45267. Phone: 513-558-2126; Fax: 513-558-4397; E-mail: susan.kasper@uc.edu

**doi:** 10.1158/0008-5472.CAN-12-1158

induces a cascade of events that result in a prometastatic phenotype in both normal and cancerous epithelial cells. Loss-of-STMN1 directly upregulates p38 signaling, which in cooperation with TGF-β promotes EMT and metastasis. Furthermore, analyses of primary epithelial cells cultured from prostate biopsies show that tissue-derived, STMN1-negative EMT-like cells are predictive of tumor stage and exhibit a metastatic phenotype *in vitro* and *in vivo*.

## Materials and Methods

### Cells and reagents

Radical retropubic prostatectomy and transurethral resection of the prostate specimens were obtained in compliance with the laws and institutional guidelines approved by the Institutional Review Board Committee of Vanderbilt University (Nashville, TN). Cells were cultured as described by Gu and colleagues (23). The DU-145 (HTB-81) and NMuMG (CRL-1636) cell lines were obtained from American Type Culture Collection. TGF-β1 (R&D Cat. 240-B) was reconstituted according to manufacturer's instructions. SB203580 hydrochloride (Tocris bioscience Cat. 1402) was reconstituted in sterile water according to manufacturer's instructions. Antibodies against E-cadherin (H-108), glyceraldehyde-3-phosphate dehydrogenase (GAPDH; A-3), vimentin (H-84) androgen receptor (AR; N-20), and prostate-specific antigen (PSA; C-19) were obtained from Santa Cruz Biotechnology. p38 (#9212), p-p38 (#9215), Smad2 (#3102), p-Smad2 (#3104), STMN1 (#3352), and DRAQ5 (#4084) were obtained from Cell Signaling. Zona occludens 1 (ZO-1) was obtained from Zymed, matrix metalloproteinase (MMP)-2 (VB3) was purchased from Thermo Scientific, and MMP-9 (Ab-3) from Oncogene. Human specific vimentin (V9) was purchased from Sigma, CD59 (CBL467) and adipophilin (PRO610102) from RDI Division of Fitzgerald Industries Intl, and antibodies to Smad3 and p-Smad3 from Rockland. Fluorescent secondary antibodies were Alexa conjugates from Invitrogen.

### qPCR

Total RNA was isolated from cells using Tri Reagent (Ambion). Random primed cDNA was synthesized using the RevertAid kit (Fermentas). STMN1 primers, 5′-AGCCCTCGGTCAAAAGAATC-3′ and 5′-TTCAAGACCTCAGCTTCATGG-3′, and ribosomal protein L32 (RPL32) primers, 5′-CAGGGTTCGTAGAAGATTCAAGGG-3′ and 5′-CTTGGAGGAAACATTGTGAGCGATC-3′ used as an internal quantitative PCR (qPCR) control, were purchased from Integrated DNA Technologies (IDT). qPCR was conducted using ABI SYBR green reaction mix and the ABI 7300 Real-Time PCR System.

### Transduction and transfection protocols

The DU-145/pLKO and DU-145/shStmn1 cell lines stably expressing pLKO/nontargeting shRNA or pLKO/STMN1 short hairpin RNA (shRNA) were generated using protocols and Lentiviral particles purchased from Sigma. DU-145 transient transfection assays were conducted using Lipofectamine 2000 (Invitrogen), STMN1 siRNA (siGENOME SMARTpools) or nontargeting siRNA control (Dharmacon). NMuMG transfection assays were conducted using pDream control vector or verified pDream-STMN1-FLAG Mission clone (Genscript). DU-145 and NMuMG cells were treated with TGF-β1 and/or SB203580 as detailed in the text later.

### Western blot analysis

Western blot analysis was conducted as described previously (1) with the modification that 50 μg total cell lysate were loaded per lane.

### Confocal imaging

Cells were cultured on poly-L-lysine coated slides using 2-well or 8-well flexiperm gaskets, fixed in ice cold methanol, rehydrated in buffered saline (PBS), and stained with primary antibodies [1:200 dilution; exceptions: anti-STMN1 (1:50); anti-vimentin (1:2,000)] using standard immunofluorescence protocols (24, 25). Images were captured using a Nikon eclipse TE 2000-U confocal microscope.

### Migration, invasion, and proliferation

Migration and invasion assays were conducted using a Neuroprobe AP48 chamber as described previously (26, 27).

### Tissue recombination assay

All animals were housed in pathogen-free units at Vanderbilt University Medical Center (Nashville, TN), and all procedures were done in compliance with Institutional Animal Care and Use Committee regulations. Tissue recombinant grafts were generated as described by Gu and colleagues (23).

### Statistical analysis

*P*-values were calculated using the Student *t* test and GraphPad PRISM4 software.

## Results

### Loss-of-STMN1 expression promotes loss of cell–cell adhesion and prometastatic behavior

We generated DU-145 prostate cancer cell lines expressing either STMN1 shRNA (termed DU-145/shSTMN1) or the nontargeting pLKO vector control (termed DU-145/pLKO) to investigate the consequences of STMN1 depletion on DU-145 epithelial cell morphology and metastatic behavior. Depletion of STMN1 expression dramatically altered epithelial cell morphology. DU-145/shSTMN1 cells appeared spindle-shaped as compared with DU-145/pLKO cells (Fig. 1A). In addition, few, if any, cell–cell adhesions remained, resulting in DU-145/shSTMN1 cells being significantly distanced from one another as compared with DU-145/pLKO cells expressing STMN1.

ZO-1 is a phosphoprotein expressed on the cytoplasmic membrane surface of intercellular tight junctions of epithelial cells (28). In control DU-145/pLKO cells, ZO-1 remained arranged in a cortical pattern at cell–cell junctions. In response to decreased STMN1 expression, ZO-1 expression decreased below detection levels (Fig. 1A). Proteins including E-cadherin form the core of adherens junctions to initiate and stabilize cell–cell adhesion (29). In response to depleted STMN1 levels, E-cadherin expression decreased below immunofluorescence detection. In contrast, vimentin expression increased, suggestive of a more mesenchymal phenotype. These changes in protein expression were confirmed by Western blot analysis (Fig. 1B and C).

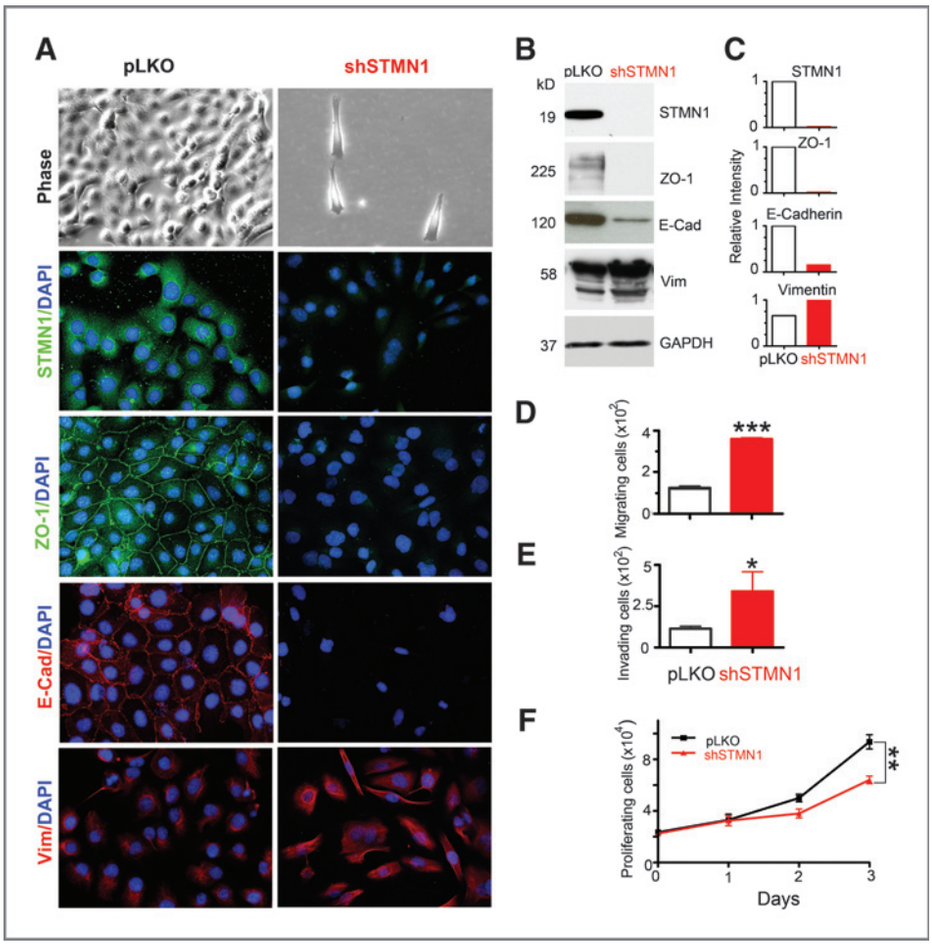


Figure 1. Loss-of-STMN1 disrupts cell–cell adhesion and induces a prometastatic phenotype. A, top, phase-contrast micrographs of DU-145/pLKO and DU-145/shSTMN1 cells. Bottom, immunofluorescence analysis using anti-STMN1, ZO-1, E-Cadherin (E-Cad), and vimentin (Vim) antibodies as indicated. Nuclei were counterstained with 4′,6-diamidino-2-phenylindole (DAPI). B, Western blot analysis of STMN1, ZO-1, E-cad, and Vim with/without STMN1 expression. C, densitometric analysis of B normalized to GAPDH. D, migration assay using uncoated polycarbonate membranes (8 μm pores). Upper chamber, serum free medium; lower chamber, medium containing 10% FBS. E, invasion assay using Matrigel-coated polycarbonate membranes (8 μm pores). The gradient was set up as in D. F, proliferation assay (trypan blue exclusion). $n \geq 3$ experiments. The values shown on graphs represent the total cell count mean ± SEM of 4 wells per treatment; *, $P < 0.05$; ***, $P < 0.0001$.

Functional hallmarks of an EMT include increased cell migration, invasion, and cell proliferation. To test whether STMN1 modulated cell migration, invasion, and/or proliferation, DU-145/shSTMN1 or DU-145/pLKO cells were plated on uncoated polycarbonate membranes and subjected to a serum gradient from serum free medium in the upper chamber to 10% FBS containing medium in the lower chamber. Both migration (Fig. 1D) and invasive activity (Fig. 1E) in DU-145/shSTMN1 cells increased 3-fold as compared with DU-145/pLKO cells. In contrast, cell proliferation rates in DU-145/shSTMN1 cells decreased (Fig. 1F).

Taken together, these observations imply that STMN1 is required in maintaining cell–cell adhesion and in suppressing metastatic characteristics.

### Loss-of-STMN1 activates p38 MAPK signaling

p38 Mitogen-activated protein kinase (MAPK) activity is reported to promote EMT, cell migration, and invasive behavior (22, 30). Control DU-145/pLKO cells expressed low basal levels of phospho-p38 (Fig. 2A), E-cadherin and ZO-1 was junctional, and vimentin expression remained at basal levels (Fig. 2B). In DU-145/shSTMN1 cells however, loss-of-STMN1 expression resulted in a 4-fold increase in p38 phosphorylation levels. In addition, an EMT-like phenotype emerged as shown by spindle-shaped morphology, increased vimentin expression, and loss of ZO-1 and E-cadherin expression (Fig. 2B).

To determine whether the phenotypic change was mediated by phospho-p38, cells were treated with the kinase inhibitor SB203580. In DU-145/shSTMN1 cells, SB203580 treatment decreased phospho-p38 expression below detection levels (Fig. 2A). Consequently, epithelial cell morphology and cell–cell adhesion were re-established as shown by re-expression and localization of ZO-1 and E-cadherin to cell–cell junctions and a concomitant decrease in vimentin expression to basal levels (Fig. 2B). In addition, SB203580 treatment inhibited

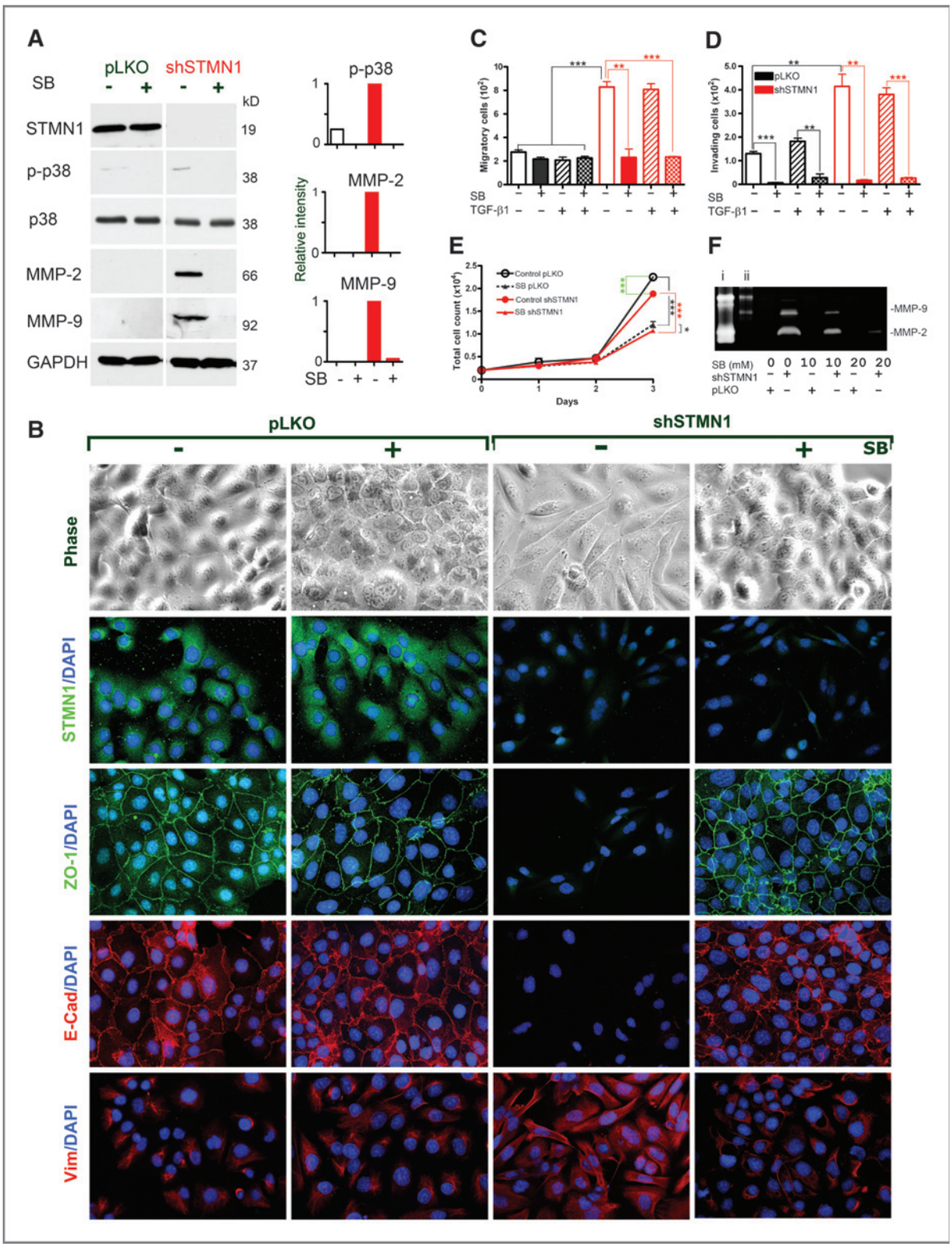


Figure 2. STMN1 regulates p38 MAPK and MMP activity. A, left, Western blot analysis of DU-145/pLKO or DU-145/shSTMN1 cells treated with/without the p38 inhibitor SB203580 (SB). Right, densitometric analysis normalized to GAPDH. B, phase contrast and immunofluorescence microscopy of cells treated with/without SB203580. C, migration assay. Upper chamber, serum free medium; lower chamber, medium containing 10% FBS. Twenty micromolar SB203580 and/or 5 ng/mL TGF-β1 were added to both chambers. D, invasion assay of cells treated with SB203580 or TGF-β1 as in C. E, proliferation assay. F, zymography for MMP-2 and MMP-9 in conditioned medium from DU-145/pLKO or DU-145/shSTMN1 cells treated without/with increasing concentrations of SB203580. Lanes i and ii contain recombinant MMP-2 and MMP-9 protein controls, respectively. $n \geq 3$ experiments. The values shown on graphs represent the total cell count mean ± SEM of 4 wells per treatment; *, $P < 0.05$; **, $P < 0.001$; ***, $P < 0.0001$.

phospho-p38–mediated migration in DU-145/shSTMN1 cells by 3.5-fold down to basal levels observed in DU-145/pLKO cells (Fig. 2C). Furthermore, cell invasion (Fig. 2D) and cell proliferation (Fig. 2E) rates in DU-145/shSTMN1 cells decreased by 15- and 2-fold, respectively. SB203580 also decreased basal phospho-p38 expression in DU-145/pLKO cells and this was sufficient to decrease invasion and proliferation rates by >8- and 2-fold, respectively; however, basal migration rates were not altered (Fig. 2C). Collectively, these observations indicate that loss-of-STMN1 directly upregulates p38 phosphorylation, which, in turn, induces a metastatic phenotype in DU-145 tumor cells.

MMPs modulate tumor microenvironment, including extracellular matrix turnover and cancer cell migration (31). Kim and colleagues reported that p38 MAPK signaling upregulated MMP-2 and MMP-9 expression (32). We determined that DU-145/pLKO cells did not express MMP-2 or MMP-9 protein (Fig. 2A). In contrast, MMP-2 and MMP-9 expression and activity were significantly induced in DU-145/shSTMN1 cells (Fig. 2A and F). MMP-2 proteinase activity seemed predominant, being 3.5-fold greater than that observed for MMP-9 (Fig. 2F). In response to SB203580 treatment, MMP-2 and MMP-9 expression were inhibited (Fig. 2A) and MMP proteinase activity decreased in a dose-dependent manner (Fig. 2F). Together, these observations imply that downregulating STMN1 promotes 38 phosphorylation, which, in turn, induces MMP-2 and MMP-9 expression and activity, resulting in extracellular matrix degradation and increased cell invasion.

Another mechanism by which p38 promotes EMT is through TGF-β–activated Smad-independent signaling (21, 22). To determine a potential role for TGF-β signaling, DU-145/shSTMN1 and DU-145/pLKO cells were treated with 5 ng/mL TGF-β1 for 48 hours. EMT morphology was not observed (data not shown) and cell migration and invasion rates were similar in DU-145/shSTMN1 and DU-145/pLKO cells (Fig. 2C and D). Furthermore, SB203580 treatment had no effect, indicating that activation of p38 seemed to be independent of short-term TGF-β1 treatment.

### Increasing STMN1 expression restores a normal epithelial cell phenotype

The nontransformed normal murine mammary gland (NMuMG) cell line has been extensively used to study EMT mechanisms (20, 33). One mechanism by which NMuMG cells undergo EMT is through TGF-β–induced activation of p38 MAP kinase (34), suggesting that NMuMG cells might express low endogenous STMN1 levels. Indeed, NMuMG cells expressed the lowest levels of STMN1 of all the cell lines tested (data not shown). Therefore, NMuMG cells were transfected with pDream/STMN1 expression vector (termed NMuMG/pSTMN1 cells) or pDream control vector (termed NMuMG/pDream cells). As expected, TGF-β1 induced EMT in control NMuMG/pDream cells within 48 hours. This morphologic change was accompanied by loss of junctional ZO-1 and E-cadherin, decreased ZO-1 and E-cadherin expression, and a concomitant increase in vimentin expression (Fig. 3A). These changes were inhibited by SB203580 treatment. In contrast, NMuMG/pSTMN1 cells retained their cobblestone-like appearance despite TGF-β1 or TGF-β1 plus SB203580 treatment. ZO-1 and E-cadherin remained junctional, and ZO-1, E-cadherin, and vimentin expression was not altered. Thus, STMN1 expression seemed sufficient to block TGF-β–mediated EMT.

Phospho-p38, MMP-2, and MMP-9 expression were also determined (Fig. 3B and C). In NMuMG/pDream cells, TGF-β1 treatment induced phospho-p38, MMP-2, and MMP-9 expression (Fig. 3B and C), and this could be inhibited with SB203580 treatment. TGF-β1 also increased cell migration (3-fold) and invasion (4-fold), which was inhibited by SB203580 treatment (Fig. 3D and E). While TGF-β1 inhibited endogenous STMN1 expression, SB203580 treatment was sufficient to re-express STMN1 with/or without addition of TGF-β1 (Fig. 3B and C). Increasing STMN1 expression was also sufficient to decrease cell proliferation (Fig. 3F).

These observations suggest that STMN1 expression is modulated by both TGF-β–dependent and TGF-β–independent activation of p38. Furthermore, restoring STMN1 expression promotes cell–cell adhesion and prevents prometastatic behavior.

### Downregulation of endogenous STMN1 expression by long-term TGF-β1 treatment

Many epithelial cell lines, including DU-145, do not undergo transition to a mesenchymal phenotype in response to short-term TGF-β1 treatment (20). This suggested that chronic exposure to TGF-β might be required to downregulate STMN1 expression and induce EMT. To test this hypothesis, native DU-145 cells were treated with 5 ng/mL TGF-β1 over a 9-day period. Few EMT-like cells were observed at 3 days of TGF-β1 treatment (Fig. 4A). At this time point, ZO-1 began to decrease, whereas vimentin increased; E-cadherin remained unchanged (Fig. 4B–D). On day 9, most, if not all, cells exhibited morphologic changes similar to those observed in DU-145/shSTMN1 cells. STMN1 expression was lost and correspondingly, E-cadherin and ZO-1 were not observed. Phospho-p38, MMP-2, and MMP-9 increased after 3 days exposure to TGF-β1 and remained high with loss-of-STMN1 expression, suggesting that their expression was regulated, in part, by TGF-β signaling. Taken together, these observations suggest that the TGF-β–mediated decrease in STMN1 expression is through indirect mechanisms.

### Decreasing STMN1 activates p38 and cooperates with TGF-β1 to enhance metastasis

To investigate a potential cooperative interaction between STMN1 and TGF-β signaling, DU-145 cells were transfected with nontargeting siRNA (NTsiRNA) or with STMN1 siRNA (siSTMN1) and treated with increasing concentrations of TGF-β1 (0–5 ng/mL). Smad2 and Smad3 were phosphorylated in a dose-dependent manner in DU-145/siSTMN1 cells similar to that observed in DU-145/NTsiRNA cells (Fig. 5A), albeit at lower levels (Fig. 5B). To determine the rate of Smad phosphorylation, cells were treated with 5 ng/mL TGF-β1 for more than 8 hours. In both cell lines, phospho-Smad2 and phospho-Smad3 increased and reached a peak at 1 to 2 hours (Fig. 5C); however, phosphorylation was prolonged in DU-145/siSTMN1

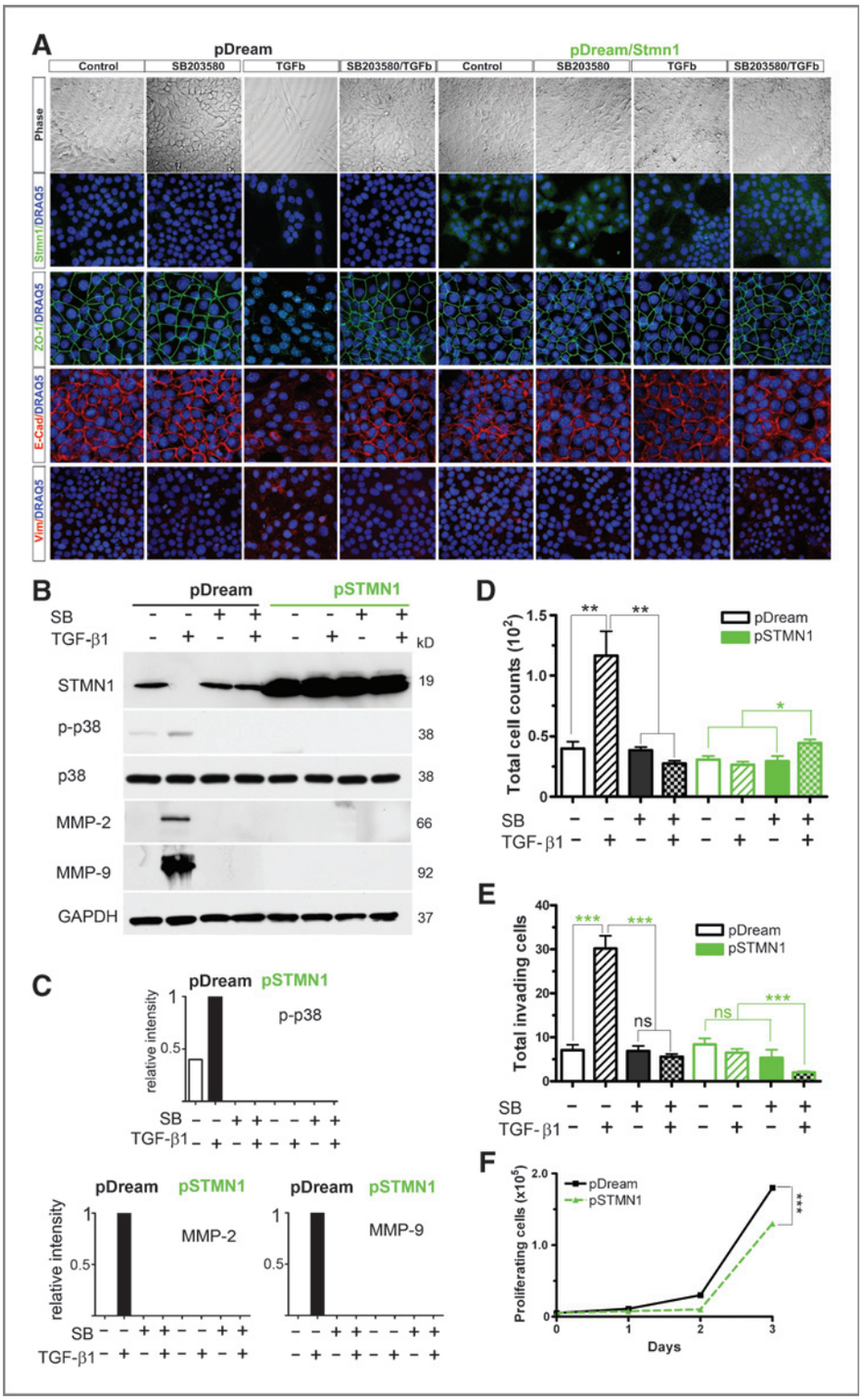


**Figure 3.** Restoring STMN1 expression prevents TGF-β-mediated EMT and inhibits the metastatic cascade. NMuMG cells were transfected with control (pDream) or STMN1 (pDream/STMN1) expression constructs and treated with/without SB203580 and/or 5 ng/mL TGF-β1 as indicated. A, phase contrast and immunofluorescence analyses. Nuclear stain, DRAQ5. B, Western blot analysis. C, densitometric analysis of B normalized to GAPDH. D, migration assay (as described in Fig. 2C). E, invasion assay. F, proliferation assay. $n \geq 3$ experiments. The values shown on graphs represent the total cell count mean ± SEM of 4 wells per treatment; *, $P < 0.05$; **, $P < 0.001$; ***, $P < 0.0001$. $n \geq 3$ experiments.

cells (Fig. 5D). Together, these data suggest that STMN1, in part, regulates the level of Smad2/3 phosphorylation as well as the length of time they are phosphorylated during TGF-β signaling.

The most dramatic response to loss of STMN1 was the 6-fold increase in phospho-p38 in untreated DU-145/siSTMN1 cells (Fig. 5C), suggesting that STMN1 could regulate p38 activity independently of TGF-β. In addition, phospho-p38 expression

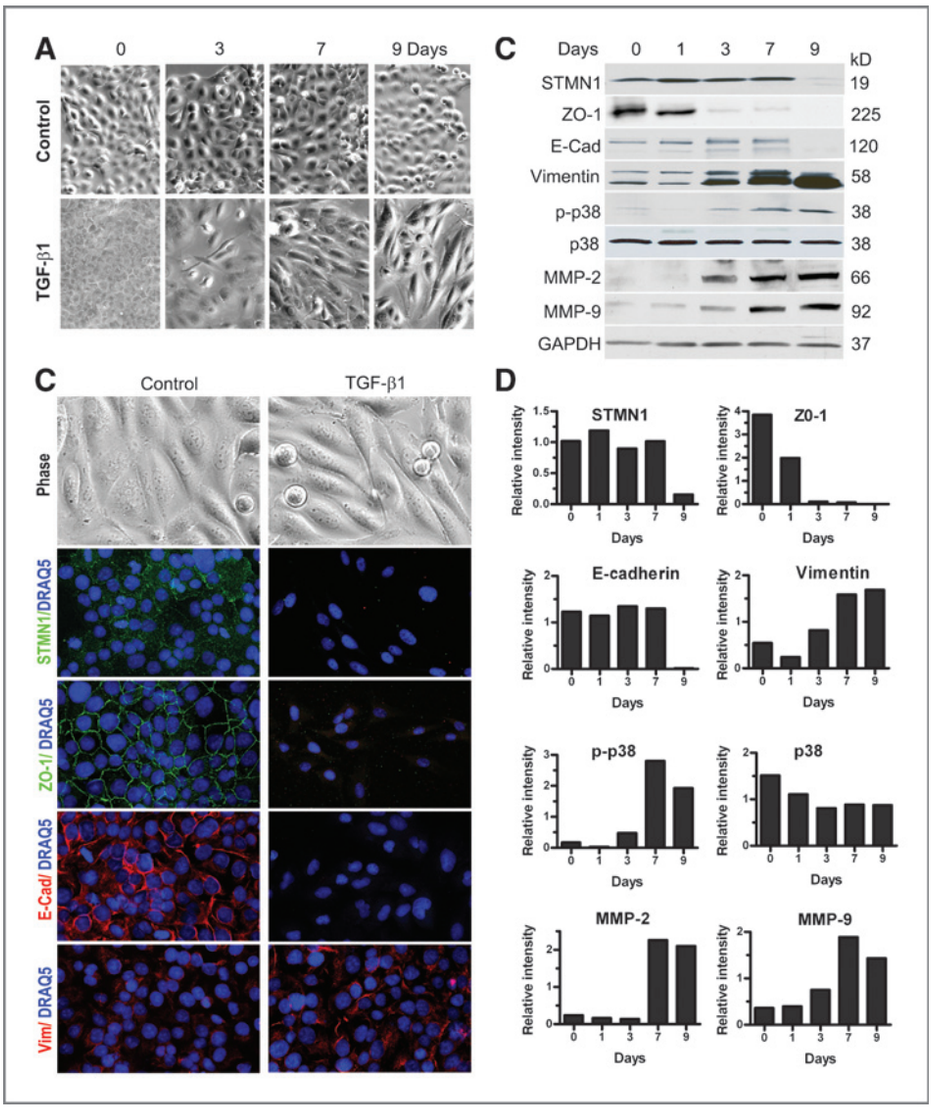


Figure 4. Long-term TGF-β1 treatment downregulates endogenous STMN1 through indirect mechanisms. DU-145 cells were treated with/without 5 ng/mL TGF-β1 for 1, 3, 7, and 9 days. A, phase contrast microscopy. B, phase contrast and immunofluorescence microscopy. C, Western blot analysis of proteins as indicated. D, densitometric analysis of C normalized to GAPDH. $n \geq 3$ experiments.

in DU-145/siSTMN1 cells was greater than that observed in DU-145/NTsiRNA cells with TGF-β1 treatment at all time points tested (Fig. 5D). These observations provide evidence that STMN1 and TGF-β1 interact cooperatively to regulate p38 MAPK signaling.

### STMN1 level and tumor-stage determine prometastatic behavior *in vitro* and *in vivo*

To determine whether EMT-like cells were present in clinical prostate cancer biopsies, primary epithelial cells were cultured from prostate biopsies ranging from benign prostatic hyperplasia (BPH) to undifferentiated adenocarcinoma (UA; ref. 23). Primary human prostate epithelial (HPE) cells exhibited typical cobblestone morphology, whereas in some cell cultures, EMT-like cells were observed (Fig. 6A and B). Few, if any, EMT-like cells were in direct cell–cell contact. As summarized in Table 1, EMT-like cell morphology was only observed in cells cultured from UA represented by Gleason scores 8 (5 of 7 specimens) and 9 (5 of 6 specimens). EMT-like cells were not observed in cell cultures from BPH, low-grade prostate cancer (prostatic intraepithelial neoplasia, PIN), or intermediate grade prostate cancer (Gleason scores 5 through 7).

Immunofluorescence analysis indicated that in UA EMT-like cells, STMN1 along with ZO-1 and E-cadherin expression greatly diminished (Fig. 6B and C), whereas vimentin levels increased (Fig. 6B). However, UA EMT-like cells continued to express the AR and the androgen-regulated protein, PSA (Fig. 6B). In addition, they retained expression of other proteins found in mature luminal secretory cells including the prostasome proteins adipophilin and CD59 (24, 25).

To determine whether UA EMT-like cells exhibited a more invasive phenotype, cell migration, invasion, and proliferation assays were conducted. Similar to that observed in DU-145/shSTMN1, DU-145/siSTMN1, and NMuMG cells, primary UA EMT-like cells exhibited increased invasion activity (14-fold; Fig. 6E) and cell proliferation decreased 2-fold (Fig. 6F); however, their migration rate resembled that of HPE cells (Fig. 6D). In contrast, HPE cells expressed STMN1 and exhibited

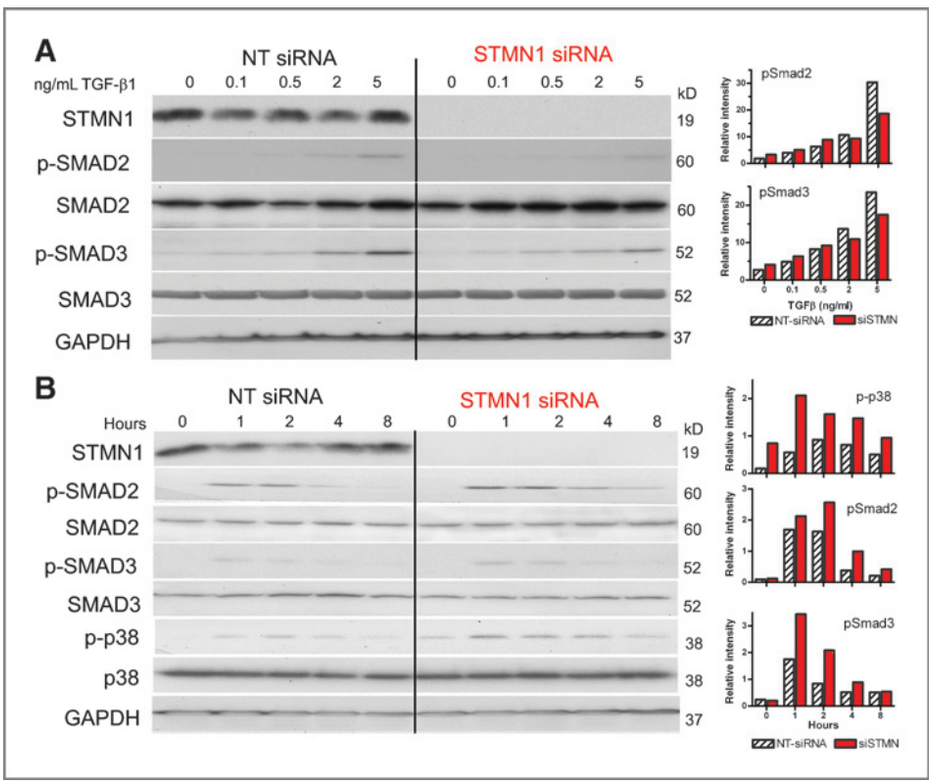


Figure 5. p38 and TGF-β signaling pathways are activated by loss-of-STMN1. A, Western blot analysis. Dose–response curve of Smad2 and Smad3 phosphorylation in DU-145 cells transiently transfected with nontargeting (NT) siRNA or STMN1 siRNA and treated for 24 hours with increasing concentrations of TGF-β1 (0–5 ng/mL). These experiments were repeated at least 3 times with similar results. The Western blot analysis and densitometry of 1 complete set are presented. B, densitometric analysis of A normalized to GAPDH. C, Western blot analysis. Time–response curve in DU-145 cells treated with 5 ng/mL TGF-β1 with increasing time (0–8 hours). D, densitometric analysis of C normalized to GAPDH. $n \geq 3$ experiments.

epithelial cell characteristics similar to those observed in control DU-145/pLKO, DU-145/NTsiRNA, and NMuMG/pDream cells.

The tissue recombination assay was used to determine whether UA EMT-like cells showed evidence of metastasis *in vivo*. Briefly, HPE or UA EMT-like cells were combined with embryonic urogenital mesenchyme cells, grafted under the renal capsule, collected after 3 months (23), and analyzed for histopathology, PSA expression, and evidence of invasive activity. Both HPE and UA EMT-like cells formed prostatic glandular structures (Fig. 6G). Furthermore, they expressed AR, PSA, and a second human-specific biomarker human mitochondria (hMT). Because PSA is human-specific, it was used to track the ability of HPE or UA EMT-like cells to migrate out of the tumor graft and into the adjacent kidney tissue. Only PSA-producing cells from UA EMT grafts, but not HPE grafts, infiltrated locally into the kidney parenchyma (Fig. 6H). Furthermore, 1 overt metastatic lesion to the lung was observed in the UA EMT group (Fig. 6I) and cells within this lesion expressed PSA, confirming that they were of human origin. The observation that only 1 overt lesion arose in a distant organ implied that while UA EMT cells could metastasize locally, additional events were likely required for a more aggressive metastatic phenotype.

## Discussion

Our findings, together with previous reports, show for the first time that STMN1 is a dual-function protein, which is involved in suppressing metastasis and in promoting oncogenesis. In normal NMuMG as well as in DU-146 and primary prostate cancer cells, STMN1 maintains cell–cell contacts, inhibits emergence of EMT, and downregulates expression and activation of MMP-2 and MMP-9. MMPs themselves also carry out dual roles in tumor progression and tumor suppression; however, this response seems to be tumor type-specific (35–37). Our study indicates that in prostate and breast epithelial cells, MMP-2 and MMP-9 promote tumor progression. As diagrammed in Fig. 7, there may be a predicative window-of-opportunity in which conserving STMN1 expression would inhibit the emergence of prometastatic disease. Identifying this stage in cancer progression would have major impact on the clinical management of epithelium-derived tumors about when targeted therapies would be most successful. Thus, the challenge is to conserve nonpathologic levels of STMN1 expression in epithelial tumors, as this would be expected to limit metastatic disease, rather than ablating STMN1, which could be expected to lead to metastatic disease.

Prostate cancer is one of the most difficult cancers to diagnose because unlike breast and colon cancer, there is no evidence that prostate cancer progresses through chronologic stages from cancer initiation to metastatic disease (38). Instead, prostate cancer is a multifocal cancer, which is evaluated by a sum of the 2 most prominent histopathologic Gleason grades (39). Gleason grades are not arranged in an order of biologic progression. Instead, they are based on physical histopathologic criteria that describe the characteristic heterogeneity of morphologies found in prostate cancer and range from 1 through 5 in which 1, 2, and 3 are considered to be low to moderate grade and 4 and 5 are considered to be

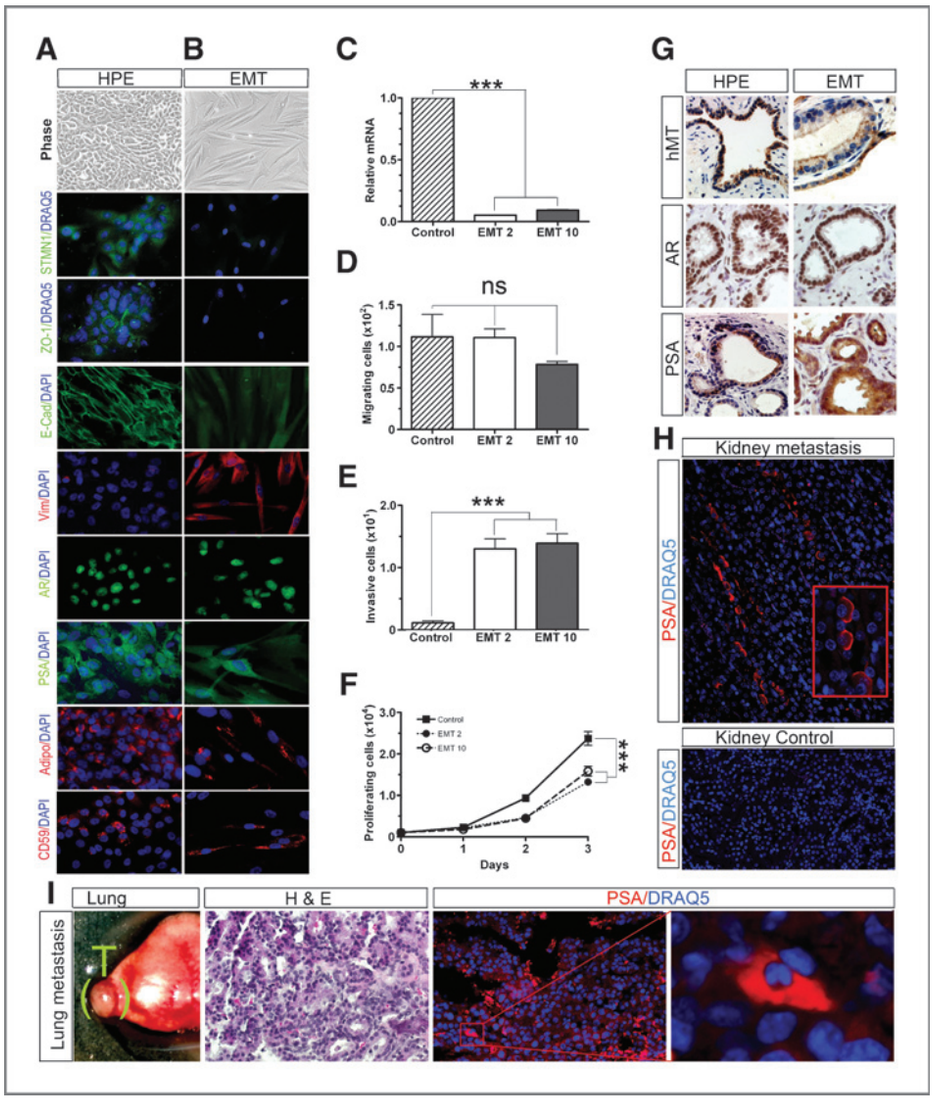


**Figure 6.** Level of STMN1 expression and tumor stage dictate EMT and prometastatic behavior *in vivo*. Primary prostate epithelial cells were cultured from prostate biopsies ranging from BPH to UA using standard epithelial cell culture conditions detailed in Gu and colleagues (23). Phase contrast microscopy of primary HPE (A) or UA EMT-like (B) cells. Immunofluorescence microscopy of STMN1, cell junction proteins (ZO-1, E-cad), mesenchymal marker (Vim), and epithelial cell markers [AR, PSA, adipophilin (Adipo), CD59]. C, qPCR analysis of STMN1 mRNA expression in HPE and EMT-like cells. STMN1 mRNA levels were normalized to ribosomal protein L32 (RPL32) mRNA. D, migration assay. E, invasion assay. F, proliferation assay. $n \geq 3$ experiments. The values shown on graphs represent the total cell count mean ± SEM of 4 wells per treatment; **, $P < 0.001$; ***, $P < 0.0001$. G–I, HPE and EMT-like tissue recombination assay. Recombinant HPE or EMT-like grafts were analyzed for expression of human-specific markers (hMT, PSA) and AR ($n = 5$). H, immunofluorescence microscopy of kidneys adjacent to recombinant grafts. Top, kidney from EMT-like graft. Bottom, kidney from HPE graft. PSA (red) was used to identify infiltrating cells from the grafts into the kidney parenchyma ($n = 4$). I, left, lung tissue showing metastatic nodule. Middle, hematoxylin & eosin (H&E). Right, immunofluorescence using anti-PSA antibody (red) and DRAQ5 (blue).

**Table 1.** A high Gleason score appears predictive of EMT. Primary prostate epithelial cells were cultured from prostate biopsies and scored for the emergence of EMT-like cells

| Diagnosis | *N* of cases | EMT | % |
|---|---|---|---|
| BPH | 23 | 0 | 0 |
| PIN | 5 | 0 | 0 |
| Gleason score 5 | 12 | 0 | 0 |
| Gleason score 6 | 33 | 0 | 0 |
| Gleason score 7 | 4 | 0 | 0 |
| Gleason score 8 | 7 | 5 | 71.4 |
| Gleason score 9 | 6 | 5 | 83.3 |
| Total | 90 | 10 | 11.1 |

high grade (38, 39). Our study presents the first biologic evidence that a histopathologic Gleason score of 8 and 9 are predictive of the emergence of EMT-like cells. Furthermore, novel observations include the ability of these cultured human EMT-like cells to develop into PSA-producing prostate tumors and their ability to metastasize locally into the surrounding kidney parenchyma *in vivo*. Interestingly, distal metastasis was limited to the discovery of 1 overt PSA(+) lesion, suggesting that tissue-derived EMT-like cells require additional events or mutations that promote aggressive spread of the disease. Whether these mutations arise in the tissue-of-origin or at a metastatic site remains to be determined.

A high Gleason score is associated with tumor spread (38). Downregulation of STMN1 expression while prostate cancer is still organ-confined could potentially be used as a prognostic biomarker for the emergence of metastatic disease. Whether STMN1 overexpression in metastatic prostate cancer lesions is associated with improved patient survival or alternatively, poor

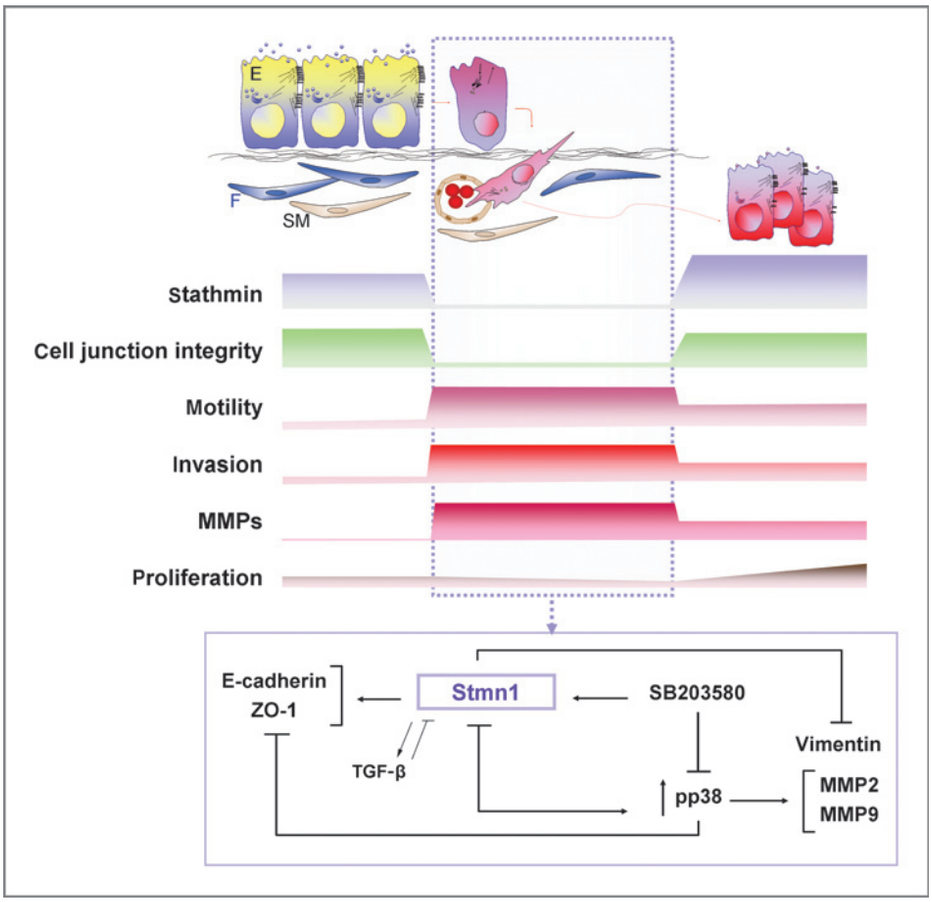


Figure 7. Schematic defining the window-of-opportunity for conserving STMN1 expression. Top, epithelial cells undergoing EMT, invading through the basement membrane into the underlying stroma, and establishing epithelial-like lesions at metastatic sites. Middle, STMN1 expression and key cellular events during EMT and metastasis. The hatched blue box summarizes the findings in this study. Bottom, mechanisms underlying the prometastatic events induced by decreased STMN1 expression. This represents the window-of-opportunity for conserving STMN1 expression to prevent metastatic spread.

clinical outcome, remains to be determined. Analysis of a large cohort of 546 colorectal cancers (stage I–IV) from 2 independent prospective cohort studies (the Nurses' Health Study and Health Care Professionals Follow-up Study) showed that STMN1 overexpression was independently associated with improved patient survival (35–37). The outcome of this study suggests that STMN1 overexpression could be a compensatory mechanism by which epithelial cells attempt to maintain cell–cell contact and normal cell function. In this event, it would be of benefit to conserve STMN1 expression and limit metastatic spread through therapeutic management. Alternatively, other studies have reported that STMN1 overexpression is an independent predictor of poor clinical outcome (35–37). While the correlation of STMN1 overexpression with poor prognosis is suggestive of oncogenic activity, this has not been confirmed in translational studies using cells derived from these cancers. Clearly, additional work needs to be done to elucidate the function(s) of STMN1 in both normal and cancer epithelium.

A challenge to the EMT hypothesis has been the inability to detect EMT cells in tissue sections from tumors (40, 41). Primary UA EMT-like cells retain expression of numerous epithelial cell-specific proteins, including PSA and prostasomal proteins. If transitioning to a mesenchymal phenotype does not abrogate epithelial cell secretory function, this may in part account for the difficulty in identifying cells-in-transition during histopathologic analysis of tissue sections.

The MAPK pathway is one of the Smad-independent mechanisms by which TGF-β regulates cell motility and EMT (34). Our study shows that loss-of-STMN1 alone is sufficient to activate p38 phosphorylation and MAPK signaling. However, TGF-β1 still increases phospho-p38 expression further in a cooperative manner. Therefore, cross-talk between STMN1 and p38 MAPK/TGF-β signaling may emerge as an important regulatory mechanism in conserving an epithelial cell phenotype.

Our study provides a crucial mechanism for STMN1-induced conservation of an epithelial cell phenotype. While STMN1 seems to be an attractive therapeutic target, its dual function as both a metastasis suppressor and oncogene would need to be considered when developing rational therapeutic modalities to treat epithelial cell-derived cancers.

## Disclosure of Potential Conflicts of Interest

No potential conflicts of interest were disclosed.

## Authors' Contributions

**Conception and design:** K. Williams, R. Ghosh, T. Case, S. Kasper
**Development of methodology:** R. Ghosh, T. Case, S. Kasper
**Acquisition of data (provided animals, acquired and managed patients, provided facilities, etc.):** K. Williams, P. Vummidi Giridhar, G. Gu, T. Case, S.M. Belcher, S. Kasper
**Analysis and interpretation of data (e.g., statistical analysis, biostatistics, computational analysis):** K. Williams, P. Vummidi Giridhar, S. Kasper

**Writing, review, and/or revision of the manuscript:** K. Williams, P. Vummidi Giridhar, S.M. Belcher, S. Kasper
**Administrative, technical, or material support (i.e., reporting or organizing data, constructing databases):** K. Williams, S. Kasper
**Study supervision:** S.M. Belcher, S. Kasper

## Grant Support

Funding for this work was provided by the National Institute of Diabetes & Digestive & Kidney Diseases (R01 DK60957 and R01 DK059142; S. Kasper), the Frances Williams Preston Laboratories of the T.J. Martell Foundation (S. Kasper), and the United States Department of Defense (W81XWH-06-1-0015; R. Ghosh).

The costs of publication of this article were defrayed in part by the payment of page charges. This article must therefore be hereby marked *advertisement* in accordance with 18 U.S.C. Section 1734 solely to indicate this fact.

Received March 27, 2012; revised July 11, 2012; accepted July 31, 2012; published OnlineFirst August 21, 2012.

## References

1. Ghosh R, Gu G, Tillman E, Yuan J, Wang Y, Fazli L, et al. Increased expression and differential phosphorylation of stathmin may promote prostate cancer progression. Prostate 2007;67:1038–52.
2. DeAngelis JT, Li Y, Mitchell N, Wilson L, Kim H, Tollefsbol TO. 2D difference gel electrophoresis analysis of different time points during the course of neoplastic transformation of human mammary epithelial cells. J Proteome Res 2011;10:447–58.
3. Ogino S, Nosho K, Baba Y, Kure S, Shima K, Irahara N, et al. A cohort study of STMN1 expression in colorectal cancer: body mass index and prognosis. Am J Gastroenterol 2009;104:2047–56.
4. Björklund P, Cupisti K, Fryknäs M, Isaksson A, Willenberg HS, Akerström G, et al. Stathmin as a marker for malignancy in pheochromocytomas. Exp Clin Endocrinol Diabetes 2010;118:27–30.
5. Ge F, Xiao CL, Bi LJ, Tao SC, Xiong S, Yin XF, et al. Quantitative phosphoproteomics of proteasome inhibition in multiple myeloma cells. PLoS ONE 2010;5:e13095.
6. Hsieh SY, Huang SF, Yu MC, Yeh TS, Chen TC, Lin YJ, et al. Stathmin1 overexpression associated with polyploidy, tumor-cell invasion, early recurrence, and poor prognosis in human hepatoma. Mol Carcinog 2010;49:476–87.
7. Mistry SJ, Atweh GF. Role of stathmin in the regulation of the mitotic spindle: potential applications in cancer therapy. Mt Sinai J Med 2002;69:299–304.
8. Steinmetz MO. Structure and thermodynamics of the tubulin–stathmin interaction. J Struct Biol 2007;158:137–47.
9. Charbaut E, Curmi PA, Ozon S, Lachkar S, Redeker V, Sobel A. Stathmin family proteins display specific molecular and tubulin binding properties. J Biol Chem 2001;276:16146–54.
10. Iancu C, Mistry SJ, Arkin S, Wallenstein S, Atweh GF. Effects of stathmin inhibition on the mitotic spindle. J Cell Sci 2001;114:909–16.
11. Gadea BB, Ruderman JV. Aurora B is required for mitotic chromatin-induced phosphorylation of Op18/stathmin. Proc Natl Acad Sci U S A 2006;103:4493–8.
12. Ringhoff DN, Cassimeris L. Stathmin regulates centrosomal nucleation of microtubules and tubulin dimer/polymer partitioning. Mol Biol Cell 2009;20:3451–8.
13. Horwitz SB, Shen HJ, He L, Dittmar P, Neef R, Chen J, et al. The microtubule-destabilizing activity of metablastin (p19) is controlled by phosphorylation. J Biol Chem 1997;272:8129–32.
14. Cassimeris L. The oncoprotein 18/stathmin family of microtubule destabilizers. Curr Opin Cell Biol 2002;14:18–24.
15. Niethammer P, Bastiaens P, Karsenti E. Stathmin–tubulin interaction gradients in motile and mitotic cells. Science 2004;303:1862–6.
16. Zarubin T, Han J. Activation and signaling of the p38 MAP kinase pathway. Cell Res 2005;15:11–8.
17. Mizumura K, Takeda K, Hashimoto S, Horie T, Ichijo H. Identification of Op18/stathmin as a potential target of ASK1-p38 MAP kinase cascade. J Cell Physiol 2006;206:363–70.
18. Betapudi V, Licate LS, Egelhoff TT. Distinct roles of nonmuscle myosin II isoforms in the regulation of MDA-MB-231 breast cancer cell spreading and migration. Cancer Res 2006;66:4725–33.
19. Li N, Jiang P, Du W, Wu Z, Li C, Qiao M, et al. Siva1 suppresses epithelial–mesenchymal transition and metastasis of tumor cells by inhibiting stathmin and stabilizing microtubules. Proc Natl Acad Sci U S A 2011;108:12851–6.
20. Brown KA, Aakre ME, Gorska AE, Price JO, Eltom SE, Pietenpol JA, et al. Induction by transforming growth factor-beta1 of epithelial to mesenchymal transition is a rare event *in vitro*. Breast Cancer Res 2004;6:R215–31.
21. Thiery JP, Acloque H, Huang RY, Nieto MA. Epithelial–mesenchymal transitions in development and disease. Cell 2009;139:871–90.
22. Zohn IE, Li Y, Skolnik EY, Anderson KV, Han J, Niswander L. p38 and a p38-interacting protein are critical for downregulation of E-cadherin during mouse gastrulation. Cell 2006;125:957–69.
23. Gu G, Yuan J, Wills M, Kasper S. Prostate cancer cells with stem cell characteristics reconstitute the original human tumor *in vivo*. Cancer Res 2007;67:4807–15.
24. Pitkänen-Arsiola T, Tillman JE, Gu G, Yuan J, Roberts RL, Wantroba M, et al. Androgen and anti-androgen treatment modulates androgen receptor activity and DJ-1 stability. Prostate 2006;66:1177–93.
25. Tillman JE, Yuan J, Gu G, Fazli L, Ghosh R, Flynt AS, et al. DJ-1 binds androgen receptor directly and mediates its activity in hormonally treated prostate cancer cells. Cancer Res 2007;67:4630–7.
26. Chen HC. Boyden chamber assay. Methods Mol Biol 2005;294:15–22.
27. Kleinman HK, Jacob K. Invasion assays. Curr Protoc Cell Biol 2001; Chapter 12:Unit 12.12.
28. Willott E, Balda MS, Fanning AS, Jameson B, Van Itallie C, Anderson JM. The tight junction protein ZO-1 is homologous to the *Drosophila* discs-large tumor suppressor protein of septate junctions. Proc Natl Acad Sci U S A 1993;90:7834–8.
29. Hartsock A, Nelson WJ. Adherens and tight junctions: structure, function and connections to the actin cytoskeleton. Biochim Biophys Acta 2008;1778:660–9.
30. Hu JY, Chu ZG, Han J, Dang YM, Yan H, Zhang Q, et al. The p38/MAPK pathway regulates microtubule polymerization through phosphorylation of MAP4 and Op18 in hypoxic cells. Cell Mol Life Sci 2010;67:321–33.
31. Kessenbrock K, Plaks V, Werb Z. Matrix metalloproteinases: regulators of the tumor microenvironment. Cell 2010;141:52–67.
32. Kim ES, Kim MS, Moon A. TGF-beta-induced upregulation of MMP-2 and MMP-9 depends on p38 MAPK, but not ERK signaling in MCF10A human breast epithelial cells. Int J Oncol 2004;25:1375–82.
33. Miettinen PJ, Ebner R, Lopez AR, Derynck R. TGF-beta induced transdifferentiation of mammary epithelial cells to mesenchymal cells: involvement of type I receptors. J Cell Biol 1994;127:2021–36.
34. Yu L, Hebert MC, Zhang YE. TGF-beta receptor-activated p38 MAP kinase mediates Smad-independent TGF-beta responses. EMBO J 2002;21:3749–59.
35. Lopez-Otin C, Matrisian LM. Emerging roles of proteases in tumour suppression. Nat Rev Cancer 2007;7:800–8.
36. Scorilas A, Karameris A, Arnogiannaki N, Ardavanis A, Bassilopoulos P, Trangas T, et al. Overexpression of matrix-metalloproteinase-9 in human breast cancer: a potential favourable indicator in node-negative patients. Br J Cancer 2001;84:1488–96.
37. Takeha S, Fujiyama Y, Bamba T, Sorsa T, Nagura H, Ohtani H. Stromal expression of MMP-9 and urokinase receptor is inversely associated with liver metastasis and with infiltrating growth in human colorectal cancer: a novel approach from immune/inflammatory aspect. Jpn J Cancer Res 1997;88:72–81.
38. Miller GJ, Torkko KC. Natural history of prostate cancer–epidemiologic considerations. Epidemiol Rev 2001;23:14–8.
39. Gleason D. The Veteran's Administration Cooperative Urologic Research Group: histologic grading and clinical staging of prostatic carcinoma. Philadelphia: Lea and Febiger; 1977. p. 171–98
40. Ledford H. Cancer theory faces doubts. Nature 2011;472:273.
41. Savagner P. The epithelial–mesenchymal transition (EMT) phenomenon. Ann Oncol 2011;21(Suppl 7):vii89–92.